Catal Lett (2008) 124:219–225
DOI 10.1007/s10562-008-9472-y

Selective Hydrogenation of Cinnamaldehyde to Hydrocinnamaldehyde over SiO_2 Supported Nickel Phosphide Catalysts

Hui Wang · Yuying Shu · Mingyuan Zheng · Tao Zhang

Received: 3 February 2008 / Accepted: 10 March 2008 / Published online: 10 April 2008

Abstract A series of SiO_2 supported transition metal (Fe, Co, Ni, Mo and W) phosphide catalysts were synthesized and tested for the selective hydrogenation of cinnamaldehyde (CMA). Among these tested catalysts, $Ni_{12}P_5/SiO_2$ and Ni_2P/SiO_2 prepared with initial Ni/P ratios of 2/1.3 and 1/1 exhibited high activity and selectivity for the conversion of CMA to hydrocinnamaldehyde (HCMA). The two nickel phosphide catalysts showed selectivity to HCMA up to 90% at a conversion of 90%. The properties of the nickel phosphide catalysts were characterized by BET surface area determinations, X-ray powder diffraction (XRD) analysis, and transmission electron microscopy (TEM). The influences of reaction temperature, hydrogen pressure, Ni/P ratio, and reduction temperature were studied in detail. For comparison, Pd/SiO_2 catalyst was also used in this reaction, and the possible reasons for the different catalytic performances of the two kinds of catalysts are presented.

Keywords Metal phosphide · $Ni_{12}P_5$ · Ni_2P · Cinnamaldehyde · Hydrogenation · Pd/SiO_2 · Hydrocinnamaldehyde

H. Wang · Y. Shu · M. Zheng · T. Zhang (✉)
State Key Laboratory of Catalysis, Dalian Institute of Chemical Physics, Chinese Academy of Sciences, 457 Zhongshan Road, Dalian 116023, China
e-mail: taozhang@dicp.ac.cn

Y. Shu
e-mail: yyshu@dicp.ac.cn

H. Wang
Graduate School of Chinese Academy of Sciences, Beijing 100039, China

1 Introduction

The chemo- and regioselective catalytic hydrogenation of α, β-unsaturated aldehydes is one of the most active research areas in catalysis research [1, 2]. The selective hydrogenation of unsaturated aldehydes to their corresponding unsaturated alcohols is highly desirable from an industrial point of view [3]. In addition, the production of the saturated aldehydes from unsaturated aldehydes has industrial and biological applications [4]. Cinnamaldehyde (CMA), one of these unsaturated aldehydes, is important in industry and its selective hydrogenation products are widely used in the perfume industry. Supported platinum [5–8], iridium [9], ruthenium [10], cobalt [11, 12], copper [13], gold [14, 15], and metal boride [16, 17] catalysts have been investigated for their selectivity to cinnamyl alcohol (CMO) in the hydrogenation of CMA. Supported ruthenium [18] and palladium [19–22] catalysts have been used in the selective hydrogenation of CMA to HCMA. Although, in some cases, the results obtained were excellent, there are still incentives for exploring new, more convenient, and economical catalysts.

Numerous methods have been reported for the preparation of metal phosphides [23], but the synthesis routes were very fussy and not environmentally friendly. By chemical reduction, amorphous nickel phosphorous alloys can be prepared simply and used as selective hydrogenation catalysts with a high activity [24, 25]. However, these amorphous catalysts are easily transformed into less active crystalline compounds [26]. Another drawback of the amorphous nickel phosphorus alloys is their selectivity to sulfur-containing compounds, which leads to deactivation [27]. Since the 1990s, a temperature-programmed reduction method has offered a simple and economical way to prepare metal phosphides [28]. These materials have a

significant capacity for avoiding the detrimental effects from sulfur and carbonization, and have attracted much attention in catalysis research. As hydrotreatment catalysts, metal phosphides have been widely used in hydrodesulfurization (HDS) and hydrodenitrogenation (HDN) [29–37]. Recently, Zhang et al. reported that MoP has excellent catalytic activity in the decomposition of hydrazine, even at a low temperature [38]. Song et al. adopted a new route to prepare supported nickel phosphide from a Ni–B amorphous alloy at low temperature. This material showed an excellent activity in the HDS of dibenzothiophene [39]. Considering the excellent catalytic performances of metal phosphides, it is logical to explore the application of metal phosphides for the catalytic hydrogenation of CMA. To our knowledge, there has been no report on this application until now.

2 Experimental

2.1 Catalyst Synthesis

SiO_2-supported phosphides (Fe_2P, CoP, Co_2P, $Ni_{12}P_5$, Ni_2P, MoP, and WP) were prepared by the temperature-programmed reduction of their corresponding phosphates, using similar procedures as reported in the literature [35]. The SiO_2 support (Qingdao Haiyang Chemical Co., Ltd, 20–40 mesh, 450 m^2/g, pore volume 1.5 mL/g) was calcined at 773 K for 3 h prior to use. In the case of the nickel phosphide catalysts (Ni/P atomic ratios of 2/1.3 and 1/1), a quantity of 0.485 or 0.746 g $(NH_4)_2HPO_4$ was dissolved in 4.2 mL distilled water, and 1.650 g $Ni(NO_3) \cdot 6H_2O$ was then added. A few drops of nitric acid were added in order to dissolve the precipitate and to form a clear solution, which was added dropwise to 3.0 g SiO_2. The precursor was dried at 393 K for 12 h and calcined at 773 K for 5 h, and then reduced in flowing hydrogen (60 ml/min/g) with the temperature ramped from room temperature to 623 K (0.06 K/s), and from 623 K to 853 or 1073 K (0.0167 K/s). To prevent the catalysts from oxidizing in air, they were passivated in 1% O_2/N_2 for 2 h at room temperature.

Pd/SiO_2 catalyst (1 wt%) was prepared by the wetness impregnation method. Impregnating solutions were prepared by dissolving 0.016 g $PdCl_2$ dissolves in 1.5 mL 1:1 HCl solution. The above solution was added dropwise to 1.0 g SiO_2 until incipient wetness. After being dried at 393 K for 6 h and calcined at 623 K for 4 h, the catalyst was reduced at 623 K for 2 h with hydrogen.

2.2 Catalyst Characterization

The X-ray diffraction (XRD) patterns of the samples were obtained with a Rigaku powder X-ray diffractometer operated at 40 kV and 100 mA using Cu–Kα monochromated radiation. The surface areas were determined using the BET method based on adsorption isotherms in a Micromeritics ASAP 2010 apparatus. The samples were characterized by adsorption of N_2 at 77 K. BET surface area (S_{BET}) and the pore size distribution of pores (PSD) were determined. Before the measurement, the samples were evacuated at 393 K for 2 h and at 523 K for 4 h. The morphology of crystal samples was examined with transmission electron microscopy (TEM) using a JEOL JEM-2000EX microscope operating at 120 kV.

2.3 Hydrogenation and Analysis

Liquid hydrogenation of CMA (Alfa Aesar, >98%) was carried out in a 300 mL stainless steel autoclave (Parr-5500) equipped with a mechanical stirrer, a hydrogen inlet, a thermocouple, a magnet stirrer, and a 4560 controller. Before use, the catalysts were pretreated in high purity H_2 at 723 K for 2 h. After the addition of 0.5 g catalyst, 3 ml CMA, and 115 mL cyclohexane, the reactor was charged and recharged 3–5 times with H_2 to exclude air. When the temperature reached the desired level (333–393 K), hydrogen was introduced to a desired pressure, and the reaction was initiated immediately by stirring the reactant vigorously (1000 rpm). During the reaction, the H_2 pressure was held constant through use of a conductor. The reaction was monitored by taking ~1.0 mL samples from the reaction mixture periodically to determine the conversion and selectivity. Generally, polar solvents will lead to many undesired products even at lower reaction temperatures [40, 41]. To avoid this, nonpolar cyclohexane was used as the solvent in this study.

An Agilent 6890 gas chromatograph with FID detector and auto injector was used for analyzing samples of reaction mixtures. The conditions for the analysis were as follows: FFAP capillary column (30 m × 0.25 mm ID), injector temperature 533 K, detector temperature 533 K, carrier gas He, 30 mL/min, and oven temperature programmed at an initial temperature of 393 K (7 min hold), followed by ramping at 3 K/min to 423 K (3 min hold), and then followed by an additional ramping at 10 K/min to the 493 K final temperature (3 min hold). The retention times of the compounds were HCMA ~12.1 min, CMA ~21.2 min, CMO ~21.6 min, and HCMO ~26.3 min.

3 Results and Discussion

3.1 Catalyst Characterization

Figure 1 shows the XRD patterns of the SiO_2 supported nickel phosphide catalysts with different Ni/P ratios and

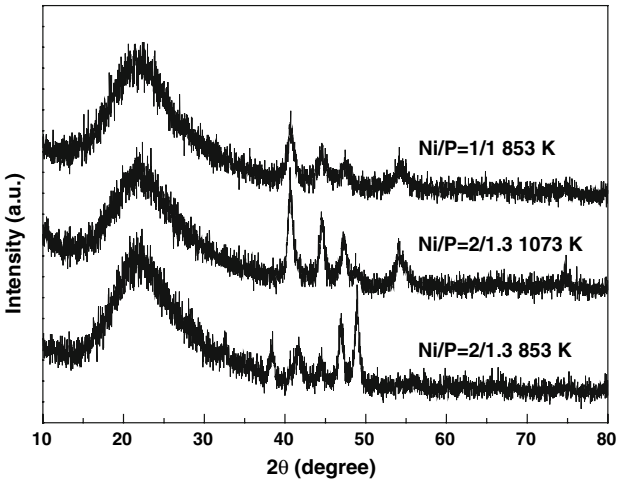

Fig. 1 XRD patterns of nickel phosphide catalysts prepared with different Ni/P ratios and reduction temperatures

reduction temperatures. When the Ni/P ratio was 2/1.3, after being reduced with H_2 at 853 K, there were intense peaks at 32.7°, 38.4°, 41.7°, 44.4°, 47.0°, and 49.0°, which were attributed to the structure of $Ni_{12}P_5$. When the Ni/P ratio was 1/1, after being reduced at 853 K with H_2, there were intense peaks at 40.7°, 44.6°, 47.4°, and 54.2° and weak peaks at 55.0° and 74.8°, which were attributed to the structure of Ni_2P. This catalyst was denoted as Ni_2P^a/SiO_2. By increasing the reduction temperature to 1073 K, the crystal structure of the nickel phosphide whose Ni/P ratio was 2/1.3 transformed from $Ni_{12}P_5$ into Ni_2P. This catalyst was denoted as Ni_2P^b/SiO_2. From the XRD results, the crystal structures of nickel phosphide were affected by the Ni/P ratio and reduction temperature.

Table 1 lists the physical properties of the two kinds of nickel phosphide catalysts and the SiO_2 support. The pure SiO_2 has a BET surface area of 450 m^2/g, a total pore volume of 0.9 cm^3/g, and an average pore diameter of 6.4 nm. It is noted that after supporting the nickel phosphide, the BET surface area and the total pore volume of SiO_2 decreased slightly but the average pore diameters did not change significantly. When the P content increased, the surface area of the catalyst decreased further.

Figure 2 shows the physisorption isotherms of the nickel phosphide catalysts. The two samples had similar adsorption-desorption isotherms, showing representative type IV isotherms, which are typical of mesoporous structures.

The TEM images in Fig. 3 clearly show that the two metal phosphide particles were distributed homogeneously on the surface of the SiO_2. The particle sizes of $Ni_{12}P_5$ centering at 10–35 nm are larger than Ni_2P^a particles with diameters of 5–20 nm. This is in good agreement with the XRD results where $Ni_{12}P_5/SiO_2$ has stronger diffraction peaks than Ni_2P^a/SiO_2.

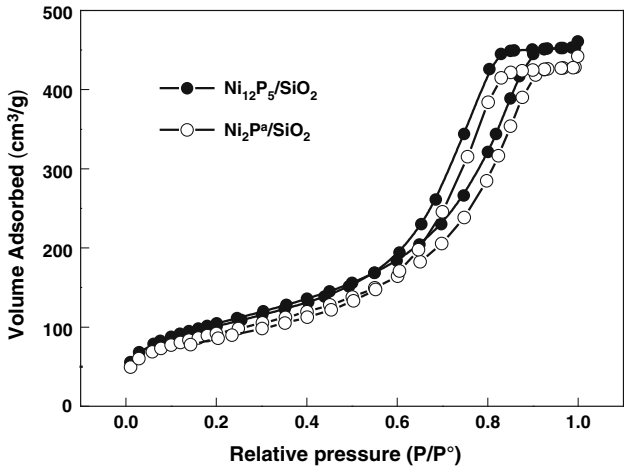

Fig. 2 N_2 physisorption isotherms of $Ni_{12}P_5/SiO_2$ and Ni_2P^a/SiO_2

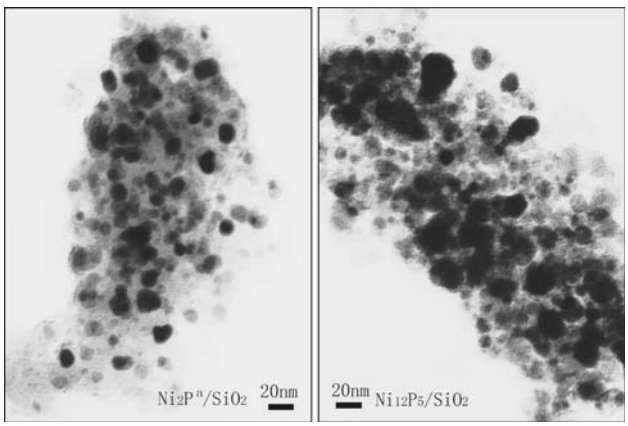

Fig. 3 TEM images of $Ni_{12}P_5/SiO_2$ and Ni_2P^a/SiO_2

Table 1 BET surface area, average pore diameter and pore volume of the nickel phosphide catalysts

Sample	Ni/P atomic ratio	Surface area (m^2/g)	Pore volume (cm^3/g)	Average pore diameter (nm)
SiO_2		455	0.9	6.4
10% $Ni_{12}P_5/SiO_2$	2:1.3	387	0.7	6.4
10% Ni_2P^a/SiO_2	1:1	334	0.7	6.3

3.2 Hydrogenation of CMA

3.2.1 Results of Different Metal Phosphide Catalysts

The reaction results for metal phosphide catalysts in the hydrogenation of CMA are summarized in Table 2. Except for the nickel phosphide catalysts, the other metal phosphide catalysts had low activity and selectivity to HCMA at 393 K and 30 bar hydrogen pressure. The selectivities to HCMA for Ni_2P^a/SiO_2 and $Ni_{12}P_5/SiO_2$ were more than 90%, but their activities were a little different under the same reaction conditions. The two kinds of nickel phosphide catalysts were prepared with the same nickel content and TPR steps, the only difference being P content. In order to clarify the influences of crystal structure and P content on the activity of nickel phosphide catalysts, Ni_2P^b/SiO_2 was used in this reaction. For these three catalysts we observed the changes in conversions and selectivities with respect to reaction time at 373 K and 30 bar.

3.2.2 Effect of Crystal structure

From Fig. 4a, under the same reaction conditions, the activity of $Ni_{12}P_5/SiO_2$ catalyst was superior to that of Ni_2P/SiO_2 prepared with Ni/P ratios of 2/1.3 and 1/1. Ni_2P^b/SiO_2 prepared with a Ni/P ratio of 2/1.3 had a better activity than Ni_2P^a/SiO_2 prepared with a Ni/P ratio of 1/1. From Fig. 4b, the selectivity to HCMA for the three catalysts also had differences within 6 h. The selectivity sequence for these catalysts was $Ni_{12}P_5/SiO_2 > Ni_2P^a/SiO_2 > Ni_2P^b/SiO_2$. By prolonging the reaction time, the conversion of CMA increased and the selectivity to HCMA became equal. Combined with the above results, the P content and crystal structure had a greater effect on the activity than on the selectivity in this reaction. After reduction when the initial Ni/P ratio was 1/1, more residual P remained in the Ni_2P^a/SiO_2 than in the Ni_2P^b/SiO_2 prepared with an initial Ni/P ratio of 2/1.3. Some of the active sites were covered with excess P which existed in the framework of the Ni_2P^a/SiO_2. It decreased the catalytic activity of Ni_2P^a/SiO_2 compared with Ni_2P^b/SiO_2. In the initial preparation step, the same Ni/P ratio was used to prepare $Ni_{12}P_5/SiO_2$ and Ni_2P^b/SiO_2. After being reduced at 1073 K, the P content in Ni_2P^b/SiO_2 was no larger than that in $Ni_{12}P_5/SiO_2$. The activity difference for these two nickel phosphide catalysts did not arise from the different P content but from the different crystal structure. According to the literature [34], the shortest Ni–Ni distances in $Ni_{12}P_5$

Table 2 Activity and selectivity data of CMA hydrogenation over different metal phosphide catalysts

Catalyst	Reaction time (min)	Conversion (%)	Selectivity (%)		
			HCMA	HCMO	CMO
10% Fe_2P/SiO_2	240	1.8	28.5	71.5	0
10% Co_2P/SiO_2	240	1.7	44.0	0	56.0
10% CoP/SiO_2	240	2.2	45.5	0	54.5
10% WP/SiO_2	240	3.4	50.0	32.4	17.6
10% MoP/SiO_2	240	3.9	40.6	54.6	4.8
10% $Ni_{12}P_5/SiO_2$	120	78.1	93.0	6.0	1.0
10% Ni_2P^a/SiO_2	120	48.2	91.2	5.8	3.0

Reaction conditions: 0.5 g catalyst, 393 K, 30 bar H_2 pressure, 3 mL CMA, 115 mL cyclohexane, and catalyst pretreated at 723 K for 2 h before testing

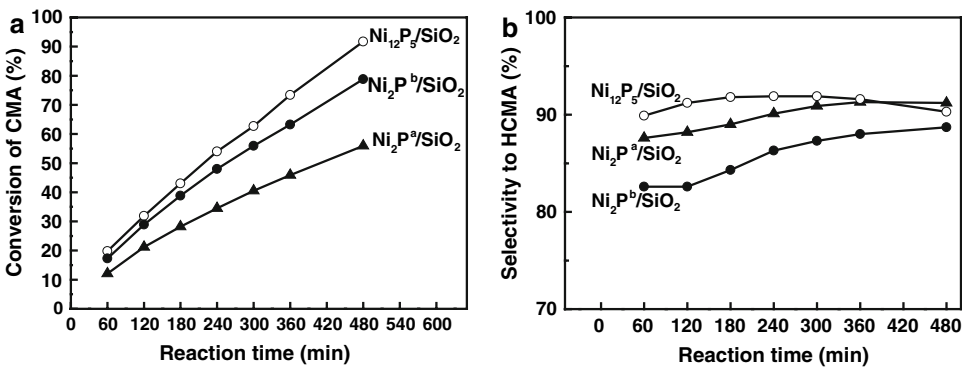

Fig. 4 Activity (**a**) and selectivity (**b**) of CMA hydrogenation over $Ni_{12}P_5/SiO_2$, Ni_2P^a/SiO_2 and Ni_2P^b/SiO_2. Reaction conditions: 0.5 g catalyst, 373 K, 30 bar H2 pressure, 3 mL CMA, 115 mL cyclohexane, and catalyst pretreated at 723 K for 2 h before testing

and Ni_2P are 2.53 and 2.61 Å, respectively, while the shortest Ni–Ni distance in Ni metal is 2.49 Å. The shorter Ni–Ni distance in $Ni_{12}P_5$ means that its properties are more metallic than those of Ni_2P. This is likely to be responsible for a higher activity of $Ni_{12}P_5/SiO_2$ than that of Ni_2P^b/SiO_2.

3.2.3 *Effects of Temperature and Hydrogen Pressure*

In addition to investigating the crystal structures and P content on the catalytic performances of nickel phosphide catalysts, we selected $Ni_{12}P_5/SiO_2$ as the catalyst to study the effects of temperature and pressure on activity and selectivity.

Table 3 contains the conversion and selectivity changes along with the reaction temperatures. With an increase in temperature the reaction rate improved significantly. From 333 to 373 K the conversion increased gently and from 373 to 393 K the increase accelerated. When the reaction temperature was 333 K, the conversion of CMA was lower, being only 6% for a reaction time of 120 min. At this conversion rate the selectivity to HCMA was only 83%, indicating the C=O bond participated in the initial reaction step, but the amount was small. When the temperature increased to 353 K and above the conversion rate was larger, the main product was HCMA, and the selectivity to HCMA was higher than 90%.

Table 4 contains the conversion and selectivity changes with different hydrogen pressures. The conversion of CMA was improved by increasing the hydrogen pressure. Selectivity to HCMA was not significantly affected by pressure.

As usual, reaction temperature and pressure are important factors for catalytic activity and selectivity, especially in a multiphase sequential reaction. With an increase in the temperature and pressure, it is important to the reaction path which bond energy is higher. In this reaction, the bond energy of the C=O double bond is larger than the C=C bond. So, as the reaction temperature and H_2 pressure increase, the amount of CMO or HCMO should increase. From the results in Tables 3 and 4, the conversion of CMA increased with increasing reaction temperature and pressure but the selectivity to HCMA remained stable. This showed that nickel phosphides were excellent catalysts for selective hydrogenation of unsaturated aldehydes to saturated aldehydes.

3.3 Hydrogenation of HCMA

For nickel phosphide catalysts with a high activity and selectivity for C=C hydrogenation, the selectivity for C=O hydrogenation was poor. In our subsequent research we used HCMA as the original material to investigate whether the nickel phosphide catalysts have the ability to hydrogenate the C=O bond. From the results in Fig. 5, $Ni_{12}P_5/SiO_2$ catalyst had an excellent activity for C=O hydrogenation. When the reaction time was 240 min, the conversion of HCMA was 88%. Compared with the results in Table 3, under the same reaction conditions the conversion of CMA was 54%. The results indicated that the $Ni_{12}P_5/SiO_2$ catalyst had a better hydrogenation ability for the C=O bond in HCMA than for the C=C bond in CMA. During the hydrogenation process of CMA, only a low

Table 3 Effect of temperature on catalytic conversion and selectivity of $Ni_{12}P_5/SiO_2$

Temperature (K)	Reaction time (min)	Conversion (%)	Selectivity (%)		
			HCMA	HCMO	CMO
333	240	5.9	83.2	6.3	10.5
353	240	25.3	90.3	4.4	5.3
373	240	54.0	91.8	5.4	2.8
393	120	78.1	93.0	6.0	1.0

Reaction conditions: 10% $Ni_{12}P_5/SiO_2$ 0.5 g, 30 bar H_2 pressure, 3 mL CMA, 115 mL cyclohexane, and catalyst pretreated at 723 K for 2 h before testing

Table 4 Effect of hydrogen pressure on catalytic conversion and selectivity of $Ni_{12}P_5/SiO_2$

H_2 pressure (bar)	Reaction time (min)	Conversion (%)	Selectivity (%)		
			HCMA	HCMO	CMO
10	240	32.1	95.1	3.0	2.1
20	240	44.9	94.7	3.5	1.8
30	240	54.0	91.8	5.4	2.8
40	240	81.7	92.2	6.1	1.7

Reaction conditions: 10% $Ni_{12}P_5/SiO_2$ 0.5 g, 373 K, 3 mL CMA, 115 mL cyclohexane, and catalyst pretreated at 723 K for 2 h before testing

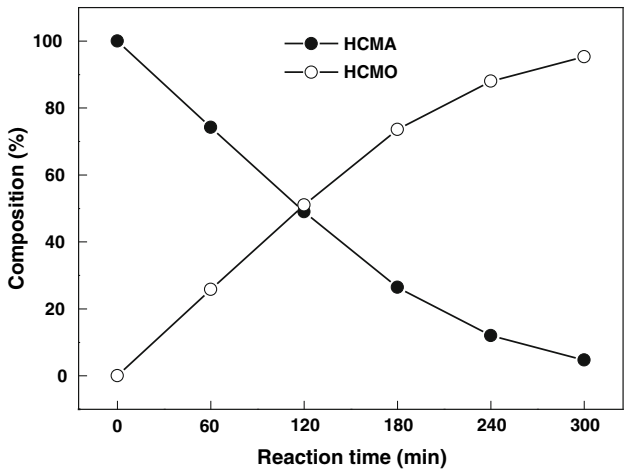

Fig. 5 Results of HCMA hydrogenation over $Ni_{12}P_5/SiO_2$. Reaction conditions: 0.5 g 10% $Ni_{12}P_5/SiO_2$, 373 K, 30 bar H_2 pressure, 3 mL HCMA, 115 mL cyclohexane, and catalyst pretreated at 723 K for 2 h before testing

percentage of C=O bonds participated in the reaction, and the produced HCMA did not hydrogenate further. A reasonable explanation is that although $Ni_{12}P_5/SiO_2$ has the ability to hydrogenate C=C and C=O bonds, this catalyst prefers hydrogenating the C=C bond rather than the C=O bond when the two double bonds exist in CMA at the same time. CMA adsorbed more strongly on the nickel phosphide surface than HCMA. When HCMA was formed, it broke away from the catalyst surface immediately, which prevented it from hydrogenating further to HCMO, so the selectivity to HCMA was kept high all through the reaction. In order to have a better understanding of the catalytic properties of the nickel phosphide catalyst in this reaction, Pd/SiO_2 catalyst was also used to make a comparison.

Figure 6a and b indicate the results of hydrogenation of CMA and HCMA over Pd/SiO_2, respectively. When the reaction time was 5 min, the conversion of CMA was as high as 80%, and the main products were HCMA and HCMO. The hydrogenation activity and selectivity of Pd/SiO_2 had a big difference compared to the nickel phosphide catalysts. When HCMA (Alfa Aesar, 97%) was the raw material, metallic Pd had no catalytic activity when supported on multi-walled carbon nanotubes at 353 K [18], so we also studied the hydrogenation of HCMA by Pd/SiO_2 at 373 K and 30 bar H_2 pressure. From the results in Fig. 6b, Pd/SiO_2 still had no activity for C=O bond hydrogenation even at the higher reaction temperature and H_2 pressure. The Pd/SiO_2 catalyst had no ability to hydrogenate the C=O bond in the HCMA, which had no C=C double bond. When hydrogenating the CMA, the C=O bond could be converted into the C-OH bond, but the selectivity to HCMA was poor. HCMA was produced by the selective hydrogenation of the C=C bond and it could not transform into HCMO over Pd/SiO_2. HCMO was produced by another path: CMA → CMO → HCMO. The reaction rate of CMO to HCMO was faster than that of CMA to CMO, so the yield of CMO was low. The difference between $Ni_{12}P_5/SiO_2$ and Pd/SiO_2 was due to $Ni_{12}P_5/SiO_2$ having a weak affinity for selective hydrogenation of the C=O bond, so the reaction producing HCMO did not happen and the selectivity to HCMA was high.

4 Conclusions

In summary, a series of economical metal phosphide catalysts have been used for the first time in the hydrogenation of CMA, and, in addition, the nickel phosphides also exhibited good activity and selectivity. P content and reduction temperature had significant effects on the crystal structure of the nickel phosphide, and they also had a large influence on the catalytic activity. With an increase in temperature and pressure the activity of the nickel phosphide catalysts improved but the selectivity to HCMA was unchanged. On the other hand, the nickel phosphide catalysts used in this experiment have a different catalytic performance from the Pd/SiO_2 catalyst. Pd/SiO_2 had a better activity and lower selectivity to HCMA compared to the nickel phosphide catalysts. The main reaction paths were CMA → HCMA and CMA → CMO → HCMO for Pd/SiO_2 catalyst. For nickel phosphides catalysts, the main reaction path was CMA → HCMA.

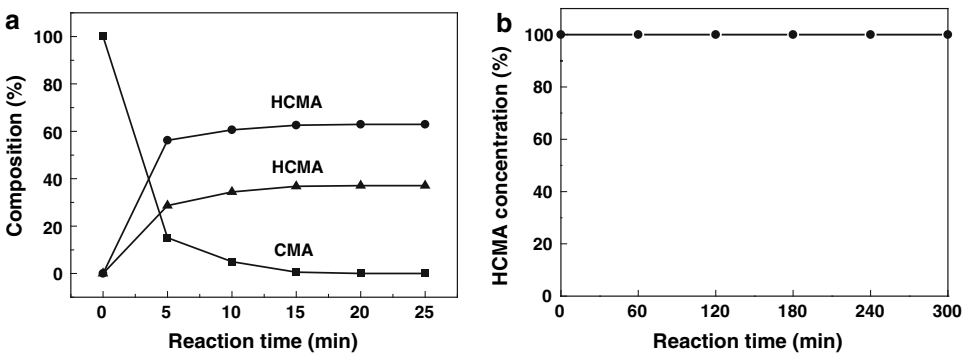

Fig. 6 Results of CMA hydrogenation (**a**) and HCMA hydrogenation (**b**) over Pd/SiO_2. Reaction conditions: 1% Pd/SiO_2, 0.2 g, 373 K, 30 bar pressure, 3 mL raw material, 115 mL cyclohexane, and catalyst pretreated at 573 K for 2 h before testing

Nickel phosphide materials will become a new class of catalysts in the selective hydrogenation of unsaturated aldehydes into saturated aldehydes.

Acknowledgment The financial support from the National Natural Science Foundation of China (No. 20573108) is gratefully acknowledged.

References

1. Bartók M, Molnár Á (1997) In: Patai S (ed) Heterogeneous catalysis hydrogenation in chemistry of functional groups, supplement A3: the chemistry of double-bonded functional groups. Wiley, New York, p 843
2. Smith GV, Notheisz F (1999) Heterogeneous catalysis in organic chemistry. Academic press, London, p 58
3. Chambers A, Jackson SD, Stirling D, Webb G (1997) J Catal 168:301
4. Castelijns AMC, Hogeweg JM, Van Nispen SPJ (1996) PCT Int Appl WO 9611898 Al, 25 April 1996, p 14
5. Szöllösi G, Török B, Baranyi L, Bartók M (1998) J Catal 179:619
6. Coq B, Brotons V, Planeix JM, de Ménorval LC, Dutartre R (1998) J Catal 176:358
7. Shirai M, Tanaka T, Arai M (2001) J Mol Catal A Chem 168:99
8. Toebes ML, Zhang YH, Hájek J, Nijhuis TA, Bitter JH, van Dillen AJ, Murzin DY, Koningsberger DC, de Jong KP (2004) J Catal 226:215
9. Breen JP, Burch R, Gomez-Lopez J, Griffin K, Hayes M (2004) Appl Catal A 268:267
10. Hájek J, Kumar N, Mäki-Arvela P, Salmi T, Murzin DY, Paseka I, Heikkilä T, Laine E, Laukkanen P, Väyrynen J (2003) Appl Catal A 251:385
11. Nitta Y, Hiramatsu Y, Imanaka T (1990) J Catal 126:235
12. Nitta Y, Ueno K, Imanaka T (1989) Appl Catal 56:9
13. Liu BJ, Lu LH, Cai TX, Iwatani K (1999) Appl Catal A 180:105
14. Bus E, Prins R, van Bokhoven JA (2007) Catal Commun 8:1397
15. Milone C, Crisafulli C, Ingoglia R, Schipilliti L, Galvagno S (2007) Catal Today 122:341
16. Li HX, Chen XF, Wang MH, Xu YP (2002) Appl Catal A 225:117
17. Chen XF, Li HX, Dai WL, Wang J, Ran Y, Qiao MH (2003) Appl Catal A 253:359
18. Lashdaf M, Tiitta M, Venäläinen T, Österholm H, Krause AOI (2004) Catal Lett 94:7
19. Pham-Huu C, Keller N, Ehret G, Charbonniere LJ, Ziessel R, Ledoux MJ (2001) J Mol Catal A: Chem 170:155
20. Pham-Huu C, Keller N, Charbonniere LJ, Ziessel BR, Ledoux MJ (2000) Chem Commun 1871
21. Zhang YK, Liao SJ, Xu Y, Yu DR (2000) Appl Catal A 192:247
22. Tessonnier JP, Pesant L, Ehret G, Ledoux MJ, Pham-Huu C (2005) Appl Catal A 288:203
23. Oyama ST (2003) J Catal 216:343
24. Deng JF, Zhang XP (1988) Appl Catal 37:339
25. Deng JF, Li HX, Wang WJ (1999) Catal Today 51:113
26. Li HX, Wang WJ, Li H, Deng JF (2000) J Catal 194:211
27. Li H, Li HX, Dai WL, Wang WJ, Fang ZG, Deng JF (1999) Appl Surf Sci 152:25
28. Li W, Dhandapani B, Oyama ST (1998) Chem Lett 207
29. Wang XQ, Clark P, Oyama ST (2002) J Catal 208:321
30. Stinner C, Prins R, Weber T (2001) J Catal 202:187
31. Robinson WRAM, van Gestel JNM, Korányi TI, Eijsbouts S, van der Kraan AM, van Veen JAR, de Beer VHJ (1996) J Catal 161:539
32. Shu YY, Oyama ST (2005) Chem Commun 1143
33. Shu YY, Oyama ST (2005) Carbon 43:1517
34. Stinner C, Tang Z, Haouas M, Weber T, Prins R (2002) J Catal 208:456
35. Zuzaniuk V, Prins R (2003) J Catal 219:85
36. Oyama ST, Wang X, Lee YK, Bando K, Requejo FG (2002) J Catal 210:207
37. Lee YK, Oyama ST (2006) J Catal 239:376
38. Cheng RH, Shu YY, Zheng MY, Li L, Sun J, Wang XD, Zhang T (2007) J Catal 249:397
39. Song LM, Li W, Wang GL, Zhang MH, Tao KY (2007) Catal Today 125:137
40. Szöllösi G, Török B, Baranyi L, Bartók M (1998) J Catal 179:619
41. Lashdaf M, Krause AOI, Lindblad M, Tiitta M, Venäläinen T (2003) Appl Catal A 241:65